The potential hazard from tsunami and seiche waves generated by large earthquakes within Lake Tahoe, California-Nevada

Gene A. Ichinose [1] and John G. Anderson [1]

Nevada Seismological Laboratory, Reno, Nevada

Kenji Satake

Geological Survey of Japan, Earthquake Research Department, Tsukuba, Japan

Rich A. Schweickert and Mary M. Lahren

University of Nevada, Department of Geological Sciences, Reno, Nevada

Abstract. We investigate the potential of local earthquakes to generate tsunamis and seiches within Lake Tahoe. We calculated the long wavelength oscillations generated by 3 hypothetical M_w > 7 earthquake scenarios for faults with normal slip directly under and outside the lake basin. The scenarios involving fault slip under the lake are the North Tahoe-Incline Village and West Tahoe-Dollar Point scenarios. The Genoa scenario involves a fault that crops out 10 km east of the lake. Faulting beneath the lake generates a tsunami followed by a seiche that continues for hours with waves as large as 3 to 10 m. The seiche potentially threatens low lying lakeside communities and lifelines. We also compare the spectral characteristics of synthetic tide gauge records with wind swell observations. The fundamental mode calculated for a seiche is consistent with the wind swell observations.

Introduction

Large prehistoric earthquakes have occurred beneath Lake Tahoe [*Hyne et al.,* 1972*; Schweickert et al.,* 1999]. Considering the size and active tectonic history of Tahoe, it is reasonable to ask if moment magnitude (M_w) 7 earthquakes can generate large devastating tsunamis and seiches. In an enclosed basin, we will refer to the tsunami as the initial wave produced by coseismic displacement from an earthquake and the seiche as the harmonic resonance within the lake.

Lake Tahoe lies in an intermontane basin bounded by normal faults [*Hyne et al.,* 1972]. The traces of these faults are mostly submerged on the lake bottom or are hidden by lacustrine and glaciofluvial deposits. A geodetic survey places 6 mm/yr of the overall Pacific-North America tectonic plate motion along the eastern Sierra near Lake Tahoe [*Thatcher et al.,* 1999]. One-half of this plate motion occurs on the faults used in this study.

A previous study by the U.S. Bureau of Reclamation investigated the potential danger to the Lake Tahoe Dam (in Tahoe City) by earthquake-induced seiche waves [*Dewey and Dise,* 1987]. They predicted a maximum wave height of 3.35 m at the dam from earthquakes similar to the scenarios in this study. Their findings led to improvements to the dam in the event of overtopping by seiche waves. A new high precision survey of the lake by *Gardner et al.,* [1998] provide high resolution bathymetry that allows for the accurate mapping of fault traces [*Schweickert et al.,* 1999] and calculation of long period wave propagation. We will utilize this new information to estimate the distribution of shoreline wave heights in greater detail than in the previous study. We compare and validate the numerical modeling results using the spectral characteristics of lake wind swells recorded by a tide gauge station.

Earthquake Scenarios and Bathymetry

We consider three hypothetical earthquake scenarios: North Tahoe-Incline Village fault (scenario A), West Tahoe-Dollar Point fault (scenario B), and Genoa fault (scenario C) [Table 1; Fig. 1]. Trenches excavated along the Genoa fault revealed two late Holocene earthquakes which occurred 575±75 and 2100±100 years ago with 3.5 to 5 m of slip per event [*Ramelli et al.,* 1999], comparable in size to the largest historical earthquakes in the Basin and Range Province [*Wells and Coppersmith,* 1994]. From these results we find it reasonable to use a maximum slip of 4 m in all of the earthquake scenarios.

Table 1. Scenario Source Parameters[1]

	u(m)	*n*	*L(km)*	*W(km)*	M_O*(dyne cm)*	M_w
A	2.63	18	36	17	4.8×10^{26}	7.0
B	2.83	24	48	17	6.9×10^{26}	7.2
C	1.92	13	65	17	6.4×10^{26}	7.1

[1]The dimensions of the fault are strike length L, dip length W with a dip of 60°. The equation used for seismic moment is, $M_O=\mu LWu$, where u is the average slip and μ is the shear modulus equal to 3×10^{11} *dyne cm*$^{-2}$. The strike length of the fault was divided into n segments and slip was tapered along strike from a maximum of 4 m at the center to 0 m at the ends of the fault using a linear slope. The slip is fixed in the dip direction.

Scenario A includes the North Tahoe-Incline Village fault zone [*Schweickert et al.,* 1999]. The northeast striking North Tahoe fault is a normal fault dipping to the southeast which is submerged under the northern portion of Lake Tahoe. Seismic reflection and marine sonar have revealed a > 10 m-high scarp displacing lake bottom sediments [*Hyne et al.,* 1972*; Schweickert et al.,* 1999]. The Incline Village fault is the on-shore continuation of the North Tahoe fault.

Scenario B includes the West Tahoe-Dollar Point fault zone [*Schweickert et al.,* 1999]. These are north-south striking normal faults. The West Tahoe fault dips to the east and is submerged from Emerald Bay to McKinney Bay. The Dollar Point fault is the northern continuation of the West Tahoe fault northward from Dollar Point. Continuity of the fault is obscured through McKinney Bay by submarine landslides, but the landslides suggests active faulting.

[1]Also at the Department of Geological Sciences, University of Nevada

Paper number 99GL11119.
000-0000/00/99GL-11119$05.00

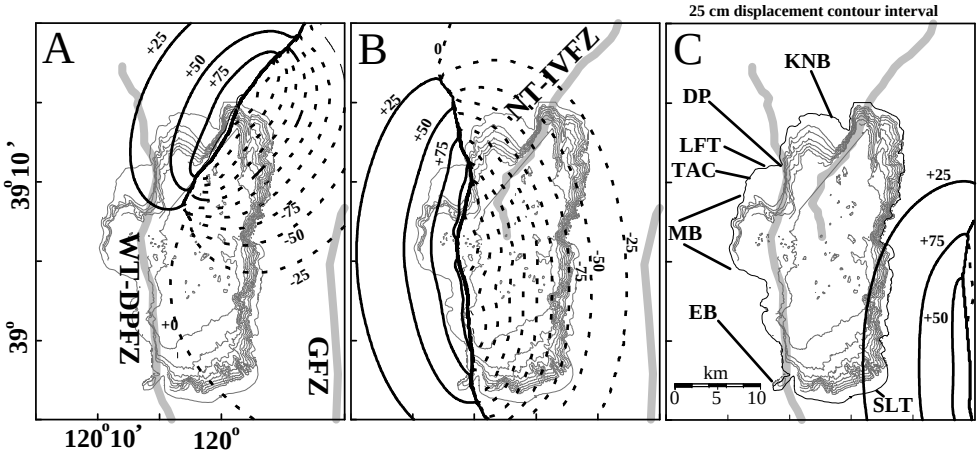

Figure 1. Scenario A, B, and C vertical component ground and lake bottom coseismic displacements. Dashed contours represent subsidence and solid contours represent uplift. Geographic locations: TAC-Tahoe City, KNB-Kings Beach, LFT-Lake Forest, SLT-South Lake Tahoe, MB-McKinney Bay, EB-Emerald Bay, DP-Dollar Point

Fig. 1 shows the modeled vertical coseismic displacement of land and lake bottom from the three scenarios. The fault traces were digitized from geologic maps into segments. Each segment was assigned a dip of 60°, typical for Basin and Range normal faults. Static coseismic displacements produced by fault slip are computed for a 3D elastic half-space from dislocation theory based on *Okada's* [1992] equations.

High resolution bathymetry and backscatter data was collected in Lake Tahoe using marine multibeam-sonar [*Gardner et al.*, 1998]. The original resolution of the bathymetry (10 m) was resampled to 2 arc-second increments. Shoreline areas not mapped by the sonar were extrapolated linearly to the modern shoreline and NOAA marine navigation maps were used to check the extrapolation. The maximum water depth is 500 m in the northern portion of the lake and the average lake elevation during the sonar survey was 1899 m, recorded by a tide gauge at Lake Forest. This elevation is used to reference the post-earthquake lake levels and simulated wave heights.

Numerical Modeling Results

A tsunami and seiche in Lake Tahoe can be treated as shallow-water long waves because the maximum water depth is much smaller than the wavelength. Wave propagation is simulated as an initial value problem. The initial lake level values were specified by assuming that the lake surface instantaneously conformed to the vertical displacement of the lake bottom while horizontal velocities were set to zero. The effect of horizontal deformation on the initial condition is neglected here and left for future work. The effect may be significant because of the coseismic displacement of the steep bathymetric slopes. For the 1994 Java Earthquake, *Tanioka and Satake* [1996] included the horizontal contribution, which resulted in a 43% increase in maximum initial vertical ground displacement and an increase in the wave amplitudes at the shoreline by as much as 30%. The predicted increase of tsunami run-up heights increased by a factor of 2. The linear hydrodynamic equations of motion were solved by the finite-difference method using a staggered grid scheme [*Satake,* 1995]. Total reflection is assumed at land-water boundaries and no wave run-up on land is considered. We use a time step of 0.2 sec to satisfy the Courant-Friedrichs-Lewy stability condition.

Scenarios were simulated for 2.5 hours elapsed from the time of the earthquake. In Scenario A, shoreline areas on the hanging wall near the fault rupture will be inundated due to permanent ground subsidence as a result of coseismic elastic rebound. Other shoreline areas would be temporarily inundated by tsunami and seiche waves. The largest amplitudes in the synthetic tide gauge records (Fig. 2) associate with the seiche rather than the tsunami. Wave amplitudes can exceed heights of 3 m within shallow bays and shores between Incline Village and Carnelian Bay, and at South Lake Tahoe with amplitudes as large as 6 m at some locations (Figs. 2 and 3). Scenario B produces a similar pattern of maximum wave amplitudes as Scenario A except that the wave amplitudes in some areas are as high as 10 m. Scenario C produces waves with average amplitudes of 0.5 m. Since static coseismic displacements decrease as the inverse cube of the distance, M_w 7 earthquakes along faults outside of the lake will not displace enough of the lake bottom to create a large seiche.

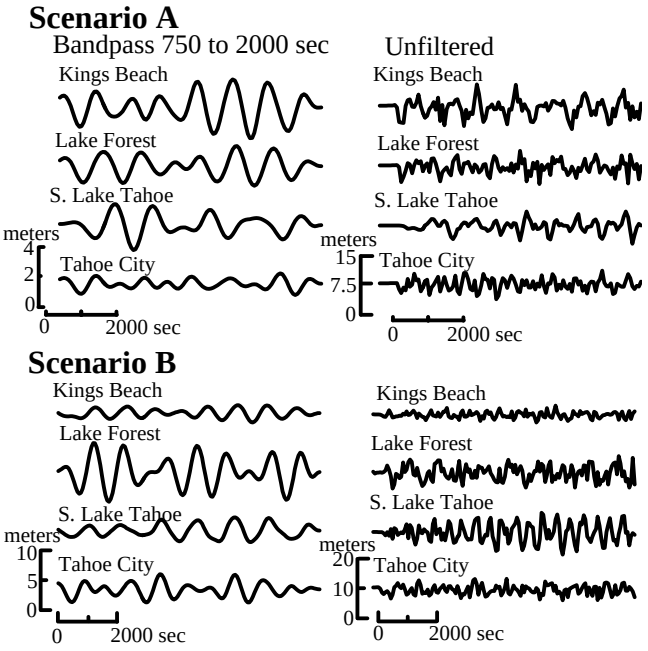

Figure 2. Filtered and unfiltered synthetic tide gauge records simulated from scenario A and B. The records are computed at the nearest shoreline grid to each location.

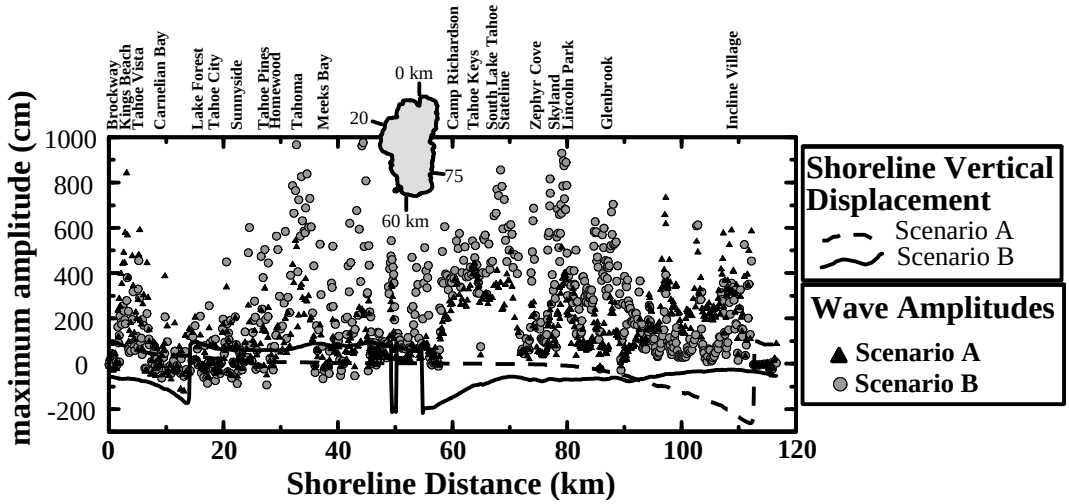

Figure 3. Predicted maximum wave amplitudes and shoreline deformation along the same shoreline track. The shoreline track distance starts from the north shore (see inset) and tracks counter-clockwise around the lake. Positive values indicate shoreline uplift and negative values are shoreline subsidence

Wind Swell Observations

A tsunami can excite a lake seiche if there is low wave damping in an enclosed basin. It is possible to identify the modes of a seiche produced by earthquakes and to compare them to observations from tide gauge records of seiches generated by wind swells. Investigators of harbor oscillations [*e.g. Thompson et al.,* 1996] have validated numerical models with wind swells. Long lasting winds can pile water up on one side of the lake. When the winds calm, the water will equilibrate and excite a seiche comparable in frequencies to those generated by earthquakes. These frequencies depend mainly on the structure of the offshore bathymetry but their excitation will depend on the direction and strength of the wind.

Wind swells were recorded at a pier in Lake Forest over the evening hours of May 15, 1999. A 2.5 hour tide gauge record, at 1 sample per *sec*, was fast Fourier transformed. Fig. (4a) shows the 3 dominant spectral peaks, of decreasing strength, at 1062, 673, and 496 sec period. We compare these spectral peaks with the Lake Forest synthetics from scenario A and B in Fig. (4b). The spectra of the synthetics from both scenarios reproduce the dominant frequency around the peak observed at 1062 sec although the spectra of the synthetics are a little more complex with a split mode at 1277 and 901 sec period. Fig (4c) shows that the synthetic tide gauge records at Kings Beach, 10 km north of Lake Forest, also provide a reasonable fit to the wind swell data with peaks at 980, 588, and 333 sec.

We estimate the periods for the fundamental and higher modes of standing waves in a rectangular basin by using the solution from the 3D wave equation with zero flow boundary conditions. The eigenperiods T_{nm} allowed are given by,

$$T_{nm} = \frac{2}{c}\left[\left(\frac{n}{L_x}\right)^2 + \left(\frac{m}{L_y}\right)^2\right]^{-\frac{1}{2}}$$

where $c = (gh)^{1/2}$ is the group velocity dependent on the square root of the water depth h and the acceleration of gravity g, L_x is the lake width, L_y is the lake length, n and m = 0,1,2,3... are the integer number of modes allowed in the x and y directions [*Sorensen*, 1993]. We calculated T_{01}, T_{10}, and T_{11} using a lake length of 35.4 km, a width of 19.2 km, and a wave group velocity of 70 m/sec assuming a constant water depth of 500 m. Fig. 5 shows the fundamental mode T_{01}, for this rectangular lake is 1011 sec and has a node in the x direction along the center of the lake. The other fundamental mode T_{10} is 548 sec and has a node in the y direction along the center of the lake. The first higher mode T_{11} is 482 sec and has two nodes which separate the lake into 4 quadrants. The

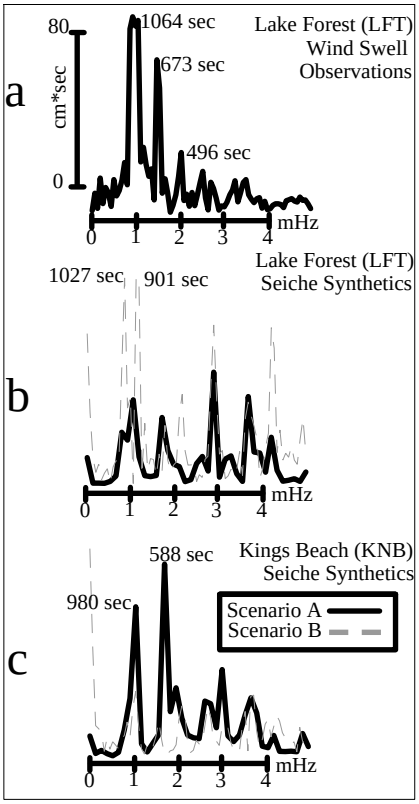

Figure 4. (a) Observed spectra of lake seiche generated by wind swells and synthetic spectra of seiche induced by earthquakes for (b) Lake Forest and (c) Kings Beach.

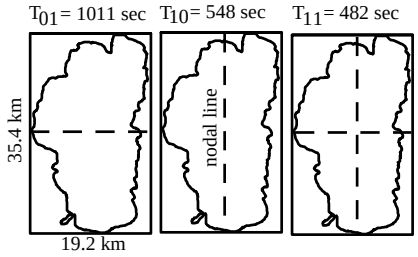

Figure 5. Fundamental (T_{01} and T_{10}) and first higher modes (T_{11}) for a rectangular lake basin with the dimensions similar to Lake Tahoe. The triangle marks the locations of two tide gauge stations in Fig. 4.

T_{01} mode, associated with the lowest fundamental mode, correlates with the dominant oscillations observed from the wind swells and also in the synthetic tide gauge records. The matches between the two other spectral peaks in the wind swell data and T_{10} and T_{11} are more questionable but we do not expect these periods to match exactly since the lake is not rectangular. Given that the fundamental seiche period is several hundred seconds, seismic surface waves, with periods of 10 to 100 sec, are not expected to generate seiche waves [*Donn*, 1964].

We do not include bottom friction and nonlinearity in the simulations for the shallow portions of the lake so the estimates of amplitudes and duration of oscillations are somewhat uncertain. However, there are some indications that the lake may be efficient in resonating because the steepness in the lake bathymetry near the east and west shores may provide total reflection. The reflection characteristics of boundaries depend on wavelength and all boundaries behave as full reflectors at longer wavelengths [*Thompson et al.*, 1996]. Excitation of free oscillations have been observed for other enclosed basins [*Satake and Shimazaki*, 1988]. A seiche in Hebgen Lake, Montana, excited by a M_w 7.5 earthquake, lasted for 11.5 hours [*Witkind*, 1960]. The duration of the seiche is important because it suggests that dangerous waves can also arrive hours after the earthquake and tsunami waves.

It is important to note that Fig. 3 represents the predicted maximum wave heights at the shore and does not reflect the wave run-up or inundation distance. Future run-up calculations will need to include nonlinear wave propagation and near shore topography.

Acknowledgments. We used GMT [Wessel and Smith, 1991] for data manipulation and graphic presentation. We thank Gerald Rockwell of the U.S. Geological Survey, Water Resources Division, for providing the tide gauge data. Animations can be viewed at http://enigma.seismo.unr.edu

References

Dewey, R. L., and K. M. Dise, Fault displacement seiche waves on inland reservoir and lakes, in the 18th joint meeting of the US-Japan Cooperative Program in Natural Resources panel, *National Bureau of Standards NBSIR 87-3540*, 289-303, 1987.

Donn, W. L., Alaskan earthquake of 27 March 1964: Remote seiche stimulation, *Science, 145*, 261-262, 1964.

Gardner, J. V., L. A. Mayer, and J. Hughes-Clarke, The bathymetry of Lake Tahoe, California-Nevada, *U.S. Geol. Surv. Open File Rep., 98-509*, 1998.

Hyne, N. J., P. Chelminski, J. E. Court, D. Gorsline, and C. R. Goldman, Quaternary history of Lake Tahoe, California-Nevada, *Geol. Soc. Am. Bull., 83*, 1435-1448, 1972.

Okada, Y., Internal deformation due to shear and tensile faults in a half-space, *Bull. Seismol. Soc. Am., 82*, 1018-1040, 1992.

Ramelli, A. R., J. W. Bell, C. M. dePolo, and J. C. Yount, Large-magnitude, late Holocene earthquakes on the Genoa fault, west-central Nevada and eastern California, *Bull. Seismol. Soc. Am., 89*, 1458-1472, 1999.

Satake, K., and K. Shimazaki, Free oscillations of the Japan Sea excited by earthquakes-I. Observations and wave theoretical approach, *Geophys. J., 93*, 451-456, 1988.

Satake, K., Linear and nonlinear computations of the 1992 Nicaragua earthquake tsunami, *PAGEOPH, 144*, 455-470, 1995.

Schweickert, R. A., M. M. Lahren, K. Smith, and R. Karlin, Preliminary fault map of the Lake Tahoe Basin, *Seismol. Res. Lett., 70*, 306-312, 1999.

Sorensen, R. M., *Basic Wave Mechanics: For Coastal and Ocean Engineers*, John Wiley and Sons, New York, 1993.

Tanioka, Y., and K. Satake, Tsunami generation by horizontal displacement of ocean bottom, *Geophys. Res. Lett., 23*, 861-864, 1996.

Thatcher, W., G. R. Foulger, B. R. Julian, J. Savrc, E. Quilty, and G. W. Bawden, Present day deformation across the Basin and Range Province, Western United States, *Science, 283*, 1714-1718, 1999.

Thompson, E. F., H. S. Chen, and L. L. Hadley, Validation of numerical model for wind waves and swells in harbors, *J. Wtrwy, Port, Coast., and Oc. Engrg., 122*, 254-257, 1996.

Wessel, P. and W. Smith, Free software helps map and display data, EOS Trans. AGU, 72, 441, 1991.

Wells, D. L., and K. J. Coppersmith, New empirical relationships among magnitude, rupture length, rupture width, rupture area, and surface displacement, *Bull. Seismol. Soc. Am., 84*, 974-1002, 1994.

Witkind, J. I., The Hebgen Lake, Montana, earthquake of August 17, 1959, in *West Yellowstone-Earthquake Area*, 31-44, 1960.

G. A. Ichinose and J. G. Anderson, Nevada Seismological Laboratory, University of Nevada, MS-174, Reno, NV 89557-0141
(e-mail: ichinose@seismo.unr.edu, jga@seismo.unr.edu)

K. Satake, Earthquake Research Department, Geological Survey of Japan, Tsukuba, 305-8567, Japan (e-mail: satake@gsj.go.jp)

R. A. Schweickert, and M. M. Lahren, Department of Geological Sciences, Unveristy of Nevada, MS-172, Reno, NV, 89557-0138
(e-mail: richschw@unr.edu, lahren@unr.edu)

(Received October 12, 1999; revised January 20, 2000;
accepted January 31, 2000.)